Fourth-Order Statistics for Blind Classification of Spatial Multiplexing and Alamouti Space-Time Block Code Signals

Yahia A. Eldemerdash, *Student Member, IEEE,* Mohamed Marey, *Member, IEEE,* Octavia A. Dobre, *Senior Member, IEEE,* George K. Karagiannidis, *Senior Member, IEEE,* and Robert Inkol, *Senior Member, IEEE*

***Abstract*—Blind signal classification, a major task of intelligent receivers, has important civilian and military applications. This problem becomes more challenging in multi-antenna scenarios due to the diverse transmission schemes that can be employed, e.g., spatial multiplexing (SM) and space-time block codes (STBCs). This paper presents a class of novel algorithms for blind classification of SM and Alamouti STBC (AL-STBC) transmissions. Unlike the prior art, we show that signal classification can be performed using a single receive antenna by taking advantage of the space-time redundancy. The first proposed algorithm relies on the fourth-order moment as a discriminating feature and employs the likelihood ratio test for achieving maximum average probability of correct classification. This requires knowledge of the channel coefficients, modulation type, and noise power. To avoid this drawback, three algorithms have been further developed. Their common idea is that the discrete Fourier transform of the fourth-order lag product exhibits peaks at certain frequencies for the AL-STBC signals, but not for the SM signals, and thus, provides the basis of a useful discriminating feature for signal classification. The effectiveness of these algorithms has been demonstrated in extensive simulation experiments, where a Nakagami-m fading channel and the presence of timing and frequency offsets are assumed.**

***Index Terms*—Signal classification, spatial multiplexing, Alamouti space-time block code, fourth-order statistics.**

I. INTRODUCTION

BLIND signal classification, an important task of intelligent receivers, finds applications in both military and commercial communications, such as electronic warfare, radio surveillance, civilian spectrum monitoring, and cognitive radio systems [1]–[7]. For example, the strategies employed by cognitive radio systems to opportunistically exploit the available spectrum require knowledge of signals in the environment to evaluate the likelihood of interfering with them [4]–[7].

Manuscript received August 27, 2012; revised January 14 and March 5, 2013. The editor coordinating the review of this paper and approving it for publication was C. da Silva.

This paper was presented in part at the IEEE International Conference on Communications, 2012 and 2013.

This work was supported in part by the Defence Research and Development Canada (DRDC).

Y. A. Eldemerdash, M. Marey, and O. A. Dobre are with the Faculty of Engineering and Applied Science, Memorial University of Newfoundland, St. John's, Canada (e-mail: {yahia.eldemerdash, mfmmarey, odobre}@mun.ca).

G. K. Karagiannidis is with the Department of Electrical and Computer Engineering, Aristotle University of Thessaloniki, 54124 Thessaloniki, Greece (e-mail: geokarag@auth.gr).

R. Inkol is with Defence Research and Development, Canada (e-mail: robert.inkol@drdc-rddc.gc.ca).

Digital Object Identifier 10.1109/TCOMM.2013.13.120629

Most previous work on blind signal classification has focused on single-input single-output scenarios [8]–[16]. However, the advent and rapid adoption of multiple-input multiple-output techniques adds a further level of complexity. These multiple antenna systems introduce new and challenging signal classification problems, such as estimation of the number of transmit antennas and the space-time code. Signal classification in the context of multiple antenna systems has been addressed by a relatively small number of papers [17]–[26]. The problems considered by these papers included the estimation of the number of transmit antennas [17], [18], modulation classification [19], [20], and the classification of linear space-time block codes (STBCs) [21]–[26].

Regarding STBC classification algorithms, they can be divided in two general categories: likelihood-based [21] and feature-based [22]–[26]. Likelihood-based algorithms calculate the likelihood function of the received signal, and employ the maximum likelihood criterion to make a decision [21]. These algorithms require channel estimation, time, block, and frequency synchronization, and knowledge of the modulation format, while they suffer from high computational complexity. In [22], [23], the space-time second-order correlation function is used as a discriminating signal feature, with the decision being made by comparing the feature with a threshold [22] or based on the minimum distance between the theoretical and estimated features [23]. Signal cyclostationarity-based features are used in [24]–[26], with the decision made based on a cyclostationarity test. Most of the previous research [22]–[25] require multiple receive antennas. However, in many practical applications, size, power, and cost constraints on the receivers may favor single receive antenna solutions for STBC classification.

In this work, the goal is to investigate the classification capability of a radio equipped with a single receive antenna. Given the assumption that either spatial multiplexing (SM) or Alamouti (AL) STBC is used by the received signal, it is shown that the fourth-order moment (FOM) and the discrete Fourier transform (DFT) of a fourth-order lag product (FOLP) can be efficiently used to blindly classify these signals[1]. Based on this result, four classification algorithms are proposed. The

[1]Note that the second-order signal statistics can be employed as discriminating features with multiple receive antennas [22]–[25]. Hence, the direct extension of a fourth-order statistic-based algorithm to multiple receive antennas makes little sense.

first algorithm is FOM-based and employs the likelihood ratio test (LRT) for decision making. Unfortunately, its practical implementation is complicated by the requirement for knowledge of the channel coefficients, modulation type, and noise power. To avoid this requirement, we propose three further algorithms which are based on the DFT of the FOLP and are referred to as FOLP-based algorithms. Furthermore, we investigate the performance of the proposed algorithms in the presence of diverse model mismatches, such as timing and frequency offsets, Doppler frequency, and spatially correlated fading.

The rest of this paper is organized as follows: Section II introduces the system model. Sections III and IV develop the FOM and FOLP-based classification algorithms, respectively. Simulation results are presented in Section V. Finally, conclusions are drawn in Section VI.

II. System Model

We consider a wireless communication system which employs linear space-time block coding with multiple transmit antennas. Each block of N_s modulated symbols is encoded to generate N_t parallel signal sequences of length L. These sequences are transmitted simultaneously with N_t antennas in L consecutive time periods [27], [28]. We denote the bth block of N_s complex symbols to be transmitted by the column vector $\mathbf{X}_b = \left[x_{b,0},...,x_{b,N_s-1}\right]^T$, with the superscript T denoting transposition. The data symbols are assumed to belong to an M-point signal constellation and consist of independent and identically distributed random variables with zero mean and second-order statistics[2] $\mathrm{E}\left\{|x|^2\right\}=1$ and $\mathrm{E}\left\{x^2\right\}=\mathrm{E}\left\{(x^*)^2\right\}=0$. Here, $\mathrm{E}\{.\}$ and $*$ denote statistical expectation and complex conjugate operations, respectively. Further, we denote the $N_t \times L$ space-time coding matrix and the $(l+1)$th column of this matrix by $\mathbb{G}(\mathbf{X}_b)$ and $\mathbb{G}_l(\mathbf{X}_b)$, $0 \le l < L$, respectively.

For SM, a block of $N_s = N_t$ symbols is transmitted simultaneously via the N_t antennas in a single time period $(L=1)$, with the coding matrix given as [27]

$$\mathbb{G}^{\mathrm{SM}}(\mathbf{X}_b) = \left[x_{b,0},...,x_{b,N_t-1}\right]^T. \tag{1}$$

For the AL-STBC, a block of two symbols $(N_s=2)$ is transmitted via two antennas $(N_t=2)$ in two consecutive time periods $(L=2)$, with the coding matrix given as [29]

$$\mathbb{G}^{\mathrm{AL}}(\mathbf{X}_b) = \begin{bmatrix} x_{b,0} & -x_{b,1}^* \\ x_{b,1} & x_{b,0}^* \end{bmatrix}, \tag{2}$$

where the rows and columns correspond to the transmit antennas and time periods, respectively.

We consider a receiver with a single antenna, and assume that the length and time alignment of the STBC blocks are unknown. Without loss of generality, we assume that the first received symbol, denoted by $r(0)$, intercepts the (k_1+1)th column, $0 \le k_1 < L$, of the bth transmitted block, denoted by $\mathbb{G}_{k_1}(\mathbf{X}_b)$. Under these assumptions, the kth intercepted symbol, $r(k)$, $k \ge 0$, is expressed as [22]

$$r(k) = \mathbf{H}\mathbf{S}(k) + w(k), \tag{3}$$

where $\mathbf{S}(k) = \mathbb{G}_p(\mathbf{X}_q)$, with $p = (k+k_1) \bmod L$, $q = b + (k+k_1) \operatorname{div} L$, and $z \bmod L$ and $z \operatorname{div} L$ denoting respectively the remainder and the quotient of the division z/L, $w(k)$ represents the complex additive white Gaussian noise (AWGN) with zero-mean and variance σ_w^2, and $\mathbf{H} = [h_0,...,h_{N_t-1}]$ is the vector of the fading channel coefficients, which are considered to be constant over the observation period.

The objective is to blindly classify the SM and AL-STBC from K received symbols, $r(k)$, $0 \le k \le K-1$, when $N_t = 2$ and a single receive antenna is available. This is formulated as a binary hypothesis testing problem: under hypothesis $\mathscr{H}_0$, the decision that SM is received is made, while the AL-STBC is selected under hypothesis $\mathscr{H}_1$.

Since lower-order statistics do not provide discriminating signal features for the SM and AL-STBC with M-ary PSK and QAM, $M \ge 4$, we resort to fourth-order statistics. Next, we show how the FOM and FOLP of the received signal can be exploited in the four proposed classification algorithms.

III. FOM-based Algorithm

The first algorithm relies on the fourth-order moment of the received signal, and applies the LRT to obtain the maximum average probability of correct classification. More specifically, we employ the fourth-order/ zero-conjugate (4,0) moment at a delay-vector $[0,0,1,1]$, defined as [30]

$$m_{r,4,0} = \mathrm{E}\left\{r^2(k)r^2(k+1)\right\}. \tag{4}$$

Note that for simplicity, the delay-vector is not specified in the moment notation. Theoretical values of this moment are subsequently derived, and the LRT is formulated based on the moment sample estimate distribution.

By using (1)-(3), the second-order statistics of data symbols, and the independence of the symbol and noise sequences, the respective expressions for $m_{r,4,0}$ of the SM and AL-STBC can be obtained as,

$$m_{r,4,0}^{\mathrm{SM}} = 0, \quad \text{and} \quad m_{r,4,0}^{\mathrm{AL}} = h_0^2 h_1^2 c_{x,4,2}, \tag{5}$$

where h_0 and h_1 are the channel coefficients, and $c_{x,4,2} = \mathrm{E}\left\{|x|^4\right\} - 2(\mathrm{E}\left\{|x|^2\right\})^2$ represents the (4,2) cumulant corresponding to the signal constellation.

In practice, we estimate $m_{r,4,0}$ based on K observed symbols (equal here to the number of samples) as [30],

$$\hat{m}_{r,4,0} = \frac{1}{K}\sum_{k=0}^{K-1} r^2(k)r^2(k+1). \tag{6}$$

Following the same procedure as [31], the sample estimate can be shown to be unbiased and asymptotically Gaussian distributed. Furthermore, by applying some mathematical manipulations to (1)-(3), and (6), we obtain the respective expressions for the variance of $\hat{m}_{r,4,0}$ for the SM and AL-STBC given by (7) and (8), where $m_{x,\alpha,\beta} = \mathrm{E}\{x^{\alpha-\beta}(x^*)^\beta\}$ represents the (α,β) moment corresponding to the signal constellation. Examples of moments and cumulants corresponding to different

[2]Results for the fourth-order statistics of SM and AL-STBC, given in Sections III and IV, are obtained under the assumption that $\mathrm{E}\left[x^2\right] = \mathrm{E}\left[(x^*)^2\right] = 0$; this corresponds to M-ary phase-shift-keying (PSK) and quadrature amplitude modulation (QAM) constellations with $M \ge 4$ [8].

$$\begin{aligned}\sigma^2_{\mathrm{SM}} = \tfrac{1}{K}\big\{&16|h_0|^4|h_1|^4 + (m_{x,4,2})^2(|h_0|^4+|h_1|^4)^2 + 8m_{x,4,2}(|h_0|^6|h_1|^2+|h_0|^2|h_1|^6)\\ &+\sigma_w^8 + 8\sigma_w^6(|h_0|^2+|h_1|^2) + 40\sigma_w^4|h_0|^2|h_1|^2 + 32\sigma_w^2(|h_0|^4|h_1|^2+|h_0|^2|h_1|^4)\\ &+18m_{x,4,2}\sigma_w^4(|h_0|^4+|h_1|^4) + 8m_{x,4,2}\sigma_w^2(|h_0|^6+|h_0|^4|h_1|^2+|h_0|^2|h_1|^4+|h_1|^6)\big\}.\end{aligned} \tag{7}$$

$$\begin{aligned}\sigma^2_{\mathrm{AL}} = \tfrac{1}{K}\big\{&(m_{x,4,2})^2(|h_0|^8+|h_1|^8) + 4(m_{x,6,3}+m_{x,4,2})(|h_0|^6|h_1|^2+|h_0|^2|h_1|^6) + \sigma_w^8\\ &+8\sigma_w^6(|h_0|^2+|h_1|^2) + 8m_{x,4,2}\sigma_w^2(|h_0|^6+|h_1|^6) + 2m_{x,4,2}\sigma_w^4(5|h_0|^4+8|h_0|^2|h_1|^2+5|h_1|^4)\\ &+4\sigma_w^2(m_{x,6,3}+5m_{x,4,2}+4)(|h_0|^4|h_1|^2+|h_0|^2|h_1|^4) + 8\sigma_w^4(|h_0|^4+3|h_0|^2|h_1|^2+|h_1|^4)\big\}.\end{aligned} \tag{8}$$

TABLE I
MOMENT AND CUMULANT VALUES FOR VARIOUS SIGNAL CONSTELLATIONS.

	QPSK	8-PSK	16-QAM	64-QAM
$m_{x,2,1} = c_{x,2,1}$	1	1	1	1
$m_{x,4,2}$	1	1	1.32	1.38
$c_{x,4,2}$	-1	-1	-0.68	-0.619
$m_{x,6,3}$	1	1	1.96	2.2
$c_{x,6,3}$	4	4	2.08	1.7972

signal constellations are provided in Table I, for $\alpha = 2,4,6$, and diverse βs [8].

Based on the statistical properties of the fourth-order moment sample estimate, $\hat{m}_{r,4,0}$, it is straightforward to write the following expressions for the probability density functions conditional on the hypothesis $\mathscr{H}_0$ (SM signal) and $\mathscr{H}_1$ (AL-STBC signal), respectively as

$$p\left(\hat{m}_{r,4,0}\,|\mathscr{H}_0\right) = \frac{1}{\pi\sigma^2_{\mathrm{SM}}}\exp\left(\frac{-|\hat{m}_{r,4,0}|^2}{\sigma^2_{\mathrm{SM}}}\right), \tag{9}$$

and

$$p\left(\hat{m}_{r,4,0}\,|\mathscr{H}_1\right) = \frac{1}{\pi\sigma^2_{\mathrm{AL}}}\exp\left(\frac{-\left|\hat{m}_{r,4,0}-h_0^2h_1^2c_{x,4,2}\right|^2}{\sigma^2_{\mathrm{AL}}}\right). \tag{10}$$

Under the assumption of equally likely hypotheses and after simple mathematical manipulations, the LRT becomes

$$\frac{|\hat{m}_{r,4,0}|^2}{\sigma^2_{\mathrm{SM}}} - \frac{\left|\hat{m}_{r,4,0}-h_0^2h_1^2c_{x,4,2}\right|^2}{\sigma^2_{\mathrm{AL}}} \underset{\mathscr{H}_0}{\overset{\mathscr{H}_1}{\gtrless}} \ln\frac{\sigma^2_{\mathrm{AL}}}{\sigma^2_{\mathrm{SM}}}. \tag{11}$$

The distributions of $\hat{m}_{r,4,0}$ conditional on hypothesis $\mathscr{H}_0$ and $\mathscr{H}_1$, given in (9) and (10), can be used to analytically determine the probability of correct classification for SM and AL-STBC signals, respectively. From the statistical communication theory [32], it follows that

$$P(\lambda=\xi\,|\xi,h_0,h_1) = 1 - Q\left(\frac{\left|h_0^2h_1^2c_{x,4,2}\right|}{\sqrt{2\sigma^2_\xi}}\right),\ \xi\in\{\mathrm{SM},\ \mathrm{AL}\}, \tag{12}$$

where λ is the estimated signal type, $P(\lambda=\xi\,|\xi,h_0,h_1), \xi\in\{\mathrm{SM},\ \mathrm{AL}\}$, is the probability of correct classification of ξ conditional on the channel coefficients, and $Q(.)$ is the Q-function, defined as $Q(x)=\int_x^\infty \frac{1}{\sqrt{2\pi}}e^{-\frac{t^2}{2}}dt$ [32]. Furthermore, the probability of correct classification, $P(\lambda=\xi\,|\xi)$, can be obtained by averaging (12) over the channel coefficients h_0 and h_1 as,

$$P(\lambda=\xi\,|\xi) = 1 - \int_0^\infty\int_0^\infty Q\left(\frac{\gamma_0^2\gamma_1^2|c_{x,4,2}|}{\sqrt{2\sigma^2_\xi}}\right)p(\gamma_0)\,p(\gamma_1)\,d\gamma_0 d\gamma_1, \tag{13}$$

where γ_i represents the magnitude of $h_i, i=0,1$. Note that, according to (7) and (8), σ^2_ξ is a function of γ_0 and γ_1. As there is no closed-form solution for (13), we used the trapezoidal numerical method described in [33] to solve the integration.

The FOM-based algorithm employs the LRT for achieving a maximum average probability of correct classification [34],

$$P_c = \frac{1}{2}\sum_{\xi\in\{\mathrm{SM},\ \mathrm{AL}\}} P(\lambda=\xi\,|\xi). \tag{14}$$

However, this requires knowledge of the channel coefficients, modulation type, and noise power. Given perfect estimates of such parameters, this result represents a performance upper bound that is useful for evaluating the performance of the other proposed algorithms. The FOM-based algorithm is summarized below.

The FOM-based algorithm

Required signal pre-processing: Blind carrier frequency and timing synchronization, blind classification of the modulation type, blind estimation of the channel coefficients, and estimation of the noise power.
Input: The observed symbols $r(k)$, $k=0,1,...,K-1$, modulation type, channel coefficients, frequency and timing information, and noise power.
- Compute the reference FOM of AL as $h_0^2h_1^2c_{x,4,2}$.
- Estimate the FOM of the received signal using (6).
- Compute σ^2_{SM} using (7).
- Compute σ^2_{AL} using (8).

if $\frac{|\hat{m}_{r,4,0}|^2}{\sigma^2_{\mathrm{SM}}} - \frac{\left|\hat{m}_{r,4,0}-h_0^2h_1^2c_{x,4,2}\right|^2}{\sigma^2_{\mathrm{AL}}} > \ln\frac{\sigma^2_{\mathrm{AL}}}{\sigma^2_{\mathrm{SM}}}$ **then**
- AL-STBC is declared present ($\mathscr{H}_1$ true).
else
- SM is declared present ($\mathscr{H}_0$ true).
end if

IV. FOLP-BASED ALGORITHMS

Based on the DFT of the FOLP at delay-vector [0,0,1,1], three classification algorithms for the SM and AL-STBC are developed. The main advantage of these algorithms is that they do not require knowledge of the channel coefficients, modulation type, and noise power.

Consider the sequence $\mathbf{y} = [y(0), y(1), ..., y(K-1)]$, with $y(k) = r^2(k)r^2(k+1)$, $k=0,1,...,K-1$. Since a random variable can be expressed as the sum of its mean and another

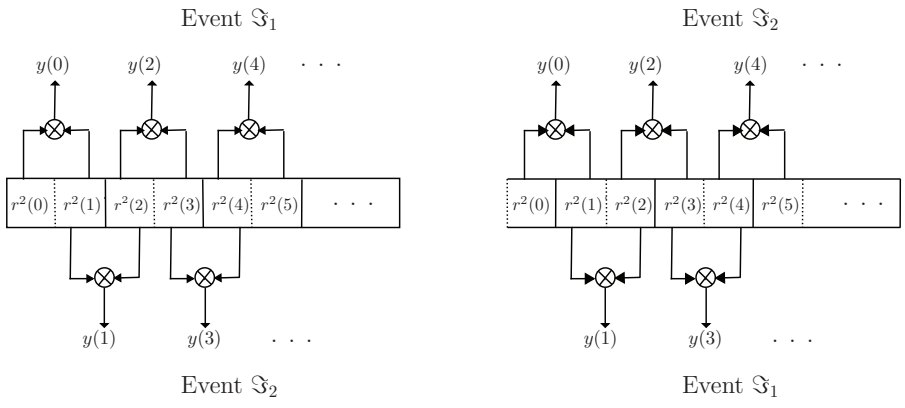

Fig. 1. Illustration of events $\Im_1$ and $\Im_2$ when (a) $r(0)$ corresponds to the beginning of the AL-STBC block, (b) $r(0)$ does not correspond to the beginning of the AL-STBC block. Solid lines are used to delimitate symbols which do not belong to the same block and dashed lines to delimitate symbols which belong to the same block.

zero-mean random variable which represents the deviation from the mean [35], $y(k)$ can be written for the SM and AL-STBC respectively as,

$$y^{\mathrm{SM}}(k) = \mathrm{E}\{y^{\mathrm{SM}}(k)\} + \psi^{\mathrm{SM}}(k), \tag{15}$$

and

$$y^{\mathrm{AL}}(k) = \mathrm{E}\{y^{\mathrm{AL}}(k)\} + \psi^{\mathrm{AL}}(k), \tag{16}$$

where $\mathrm{E}\{y^{\xi}(k)\}$ is the mean of $y^{\xi}(k)$, and $\psi^{\xi}(k)$ is its deviation from the mean, $\xi \in \{\mathrm{SM}, \mathrm{AL}\}$.

Based on (2)-(5), one can easily show that $\mathrm{E}\{y^{\mathrm{AL}}(k)\}$ equals $2h_0^2h_1^2c_{x,4,2}$ when $r(k)$ and $r(k+1)$ belong to the same transmitted data block (event $\Im_1$), and zero when they do not (event $\Im_2$). The difference between events $\Im_1$ and $\Im_2$ is illustrated in Fig. 1. Apparently, under the event $\Im_1$, $\mathrm{E}\{y^{\mathrm{AL}}(k)\}$ is a constant, $C = 2h_0^2h_1^2c_{x,4,2}$, which depends on the modulation type and channel coefficients. Further, $\psi^{\mathrm{AL}}(k)$ can be considered as a noise component that hides the presence of C if $y^{\mathrm{AL}}(k)$ is received. Furthermore, based on (1), (3)-(5), it is easy to show that $\mathrm{E}\{y^{\mathrm{SM}}(k)\} = 0$; thus, $\psi^{\mathrm{SM}}(k)$ can be seen as a noise component which hides the absence of C if $y^{\mathrm{SM}}(k)$ is received. In the absence of such noise components, i.e., $\psi^{\mathrm{SM}}(k) = \psi^{\mathrm{AL}}(k) = 0$, the FOLP sequence for the AL-STBC code would be either $[C,0,C,0,C,0,C,...]$ or $[0,C,0,C,0,C,0,...]$, depending on whether or not $r(0)$ and $r(1)$ correspond to the same data block, and the FOLP sequence for SM would be $[0,0,0,0,0,0,...]$. The following discussion shows how this property can be exploited as a feature for distinguishing between the SM and AL-STBC in the frequency domain.

Let $\mathbf{Y} = [Y(0), Y(1), ..., Y(K-1)]$ denote the K-point DFT[3] of $\mathbf{y}$, with

$$Y(n) = \frac{1}{\sqrt{K}} \sum_{k=0}^{K-1} y(k) e^{-j2\pi kn/K}, \qquad n = 0, 1, ..., K-1. \tag{17}$$

By replacing (15) and (16) in (17), it follows that

$$Y^{\mathrm{SM}}(n) = \Psi^{\mathrm{SM}}(n), n = 0, 1, ..., K-1, \tag{18}$$

and

$$Y^{\mathrm{AL}}(n) = \begin{cases} \mathscr{E} + \Psi^{\mathrm{AL}}(n), & n = 0, K/2, \\ \Psi^{\mathrm{AL}}(n), & \text{otherwise}, \end{cases} \tag{19}$$

where $\Psi^{\mathrm{SM}}(n)$ and $\Psi^{\mathrm{AL}}(n)$ represent the DFT of $\psi^{\mathrm{SM}}(k)$ and $\psi^{\mathrm{AL}}(k)$, respectively. $\mathscr{E} = \frac{\sqrt{K}}{2}C$ if $r(0)$ and $r(1)$ belong to the same transmitted data block, and $\mathscr{E} = \pm\frac{K-2}{2\sqrt{K}}C \approx \pm\frac{\sqrt{K}}{2}C$ otherwise; the plus sign corresponds to $n = 0$ and the minus sign to $n = K/2$. Clearly, (18) and (19) indicate that $|Y(n)|$ does not exhibit peaks for SM, but it does for the AL-STBC at $n = 0, K/2$.

From (17), $Y(n)$ is composed of a large number of contributions when K is large. Consequently, the central limit theorem indicates that $Y(n)$ should have a Gaussian distribution when K tends to infinity. A closer look at (17) and (18) reveals that the asymptotic distribution of $Y(n)$, $n = 0, \cdots K-1$, for SM is Gaussian with zero mean. In addition, further consideration of (17) and (19) indicates that the asymptotic distribution of $Y(n)$ for the AL-STBC is also Gaussian with zero mean at $n = 0, \cdots K-1$, $n \neq 0, K/2$, and non-zero mean, $\mathscr{E}$, at $n = 0, K/2$.

The following subsections describe the development of the decision criteria that form the basis of the three proposed FOLP-based classification algorithms.

A. FOLP-A classification algorithm

The basic idea of the FOLP-A classification algorithm is to test for the existence of peaks in $|Y(n)|$, either at $n = 0$ or $n = K/2$, as follows. We define n_1 as the value of n that maximize $|Y(n)|$,

$$n_1 = \arg\max_n |Y(n)|, \qquad n = 0, 1, ..., K-1. \tag{20}$$

If $n_1 \in \{0, K/2\}$, the AL-STBC is declared present ($\mathscr{H}_1$ true); otherwise, SM is declared present ($\mathscr{H}_0$ true). A summary of the proposed FOLP-A algorithm is provided below.

[3]Note that, without loss of generality, K is assumed to be even.

The FOLP-A algorithm

Required signal pre-processing: Blind carrier frequency and timing synchronization.
Input: The observed symbols $r(k)$, $k = 0,1,...,K-1$, and frequency and timing information.
- Compute the fourth-order lag product $y(k) = r^2(k)r^2(k+1)$.
- Compute $Y(n)$ using (17).
- $n_1 = \arg\max_n |Y(n)|, \quad n = 0,1,...,K-1.$
if $n_1 \in \{0, K/2\}$ **then**
- AL-STBC is declared present ($\mathscr{H}_1$ true).
else
- SM is declared present ($\mathscr{H}_0$ true).
end if

B. FOLP-B classification algorithm

The FOLP-B classification algorithm exploits the statistical properties of $|Y(n)|$, $n = 0, \cdots, K-1$, to decide whether $|Y(n)|$ exhibits a peak either at $n = 0$ or $n = K/2$. Note that $\mathscr{E}$ depends on the modulation format and the channel coefficients, which are unknown at the receiver; as such, the statistics of $Y(n=0)$ and $Y(n=K/2)$ for the Alamouti code are unknown, as well. The basic idea behind this algorithm is to set a threshold, ε, to achieve a given probability of false alarm[4], P_{fa}. As a consequence, if either $|Y(n=0)|$ or $|Y(n=K/2)|$ is greater than ε, the AL-STBC is declared present ($\mathscr{H}_1$ true); if not, SM is declared present ($\mathscr{H}_0$ true). The problem is to set this threshold to yield the desired value of P_{fa}. Since the distributions of $Y(n=0)$ and $Y(n=K/2)$ for the SM are Gaussian with zero mean, the distributions of $|Y(n=0)|$ and $|Y(n=K/2)|$ are Rayleigh. Accordingly, the probability of false alarm, P_{fa}, can be expressed as

$$P_{fa} = \int_{\varepsilon}^{\infty} \frac{2x}{\Omega} e^{\frac{-x^2}{\Omega}} dx, \tag{21}$$

where Ω represents the second-order moment which characterizes the Rayleigh distribution. Hence, ε can be calculated as

$$\varepsilon = \sqrt{-\Omega \ln\left(P_{fa}\right)}. \tag{22}$$

In practice, an estimate of Ω is employed, which is obtained as

$$\hat{\Omega} = \frac{1}{K-2}\left[\sum_{n=0, n\neq 0, K/2}^{K-1} |Y(n)|^2\right]. \tag{23}$$

Note that $|Y(0)|$ and $|Y(K/2)|$ are excluded, as these have a different distribution if the AL-STBC is present (hypothesis $\mathscr{H}_1$).

Fig. 2 presents the distribution of $|Y(n)|$ with $n \neq 0, K/2$ for the AL-STBC with quadrature PSK (QPSK) modulation, $K = 2048$, and 20 dB signal-to-noise ratio (SNR). We also show the theoretical Rayleigh distribution with $\Omega = \hat{\Omega}$. Since the simulation and theoretical results are in reasonable agreement, the assumption that $|Y(n)|$ with $n \neq 0, K/2$ has a Rayleigh distribution is validated. Similar results are obtained for $|Y^{\mathrm{SM}}(n)|$, but are not shown due to space considerations.

[4]The probability of false alarm is defined as the probability of incorrectly deciding that a statistically significant peak is present.

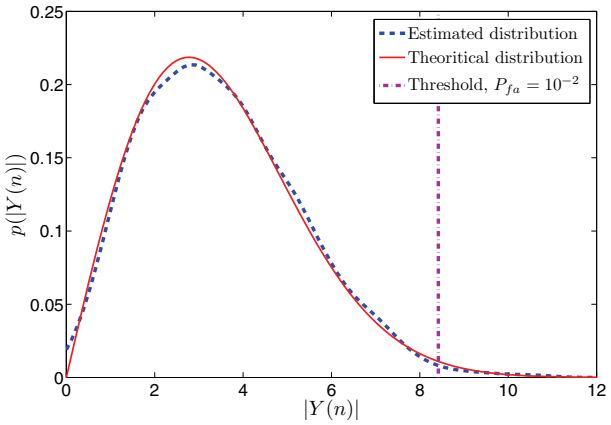

Fig. 2. Distribution of $|Y(n)|$, $n \neq 0, K/2$, for the AL-STBC with QPSK modulation and $K = 2048$, at SNR=20 dB over Nakagami-m channel, $m = 3$.

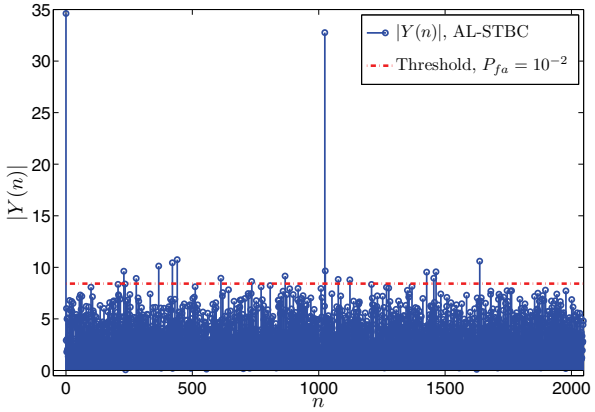

Fig. 3. $|Y(n)|$ for the AL-STBC with QPSK modulation and $K = 2048$, at SNR = 20 dB over Nakagami-m channel, $m = 3$.

Furthermore, Fig. 3 depicts $|Y(n)|$ for the AL-STBC as a function of n, along with the threshold ε associated to the probability of false alarm $P_{fa} = 10^{-2}$. Note that the value of $|Y(n)|$ is greater than ε for $n = 0, K/2$, as expected. A summary of the proposed FOLP-B is provided below.

The FOLP-B algorithm

Required signal pre-processing: Blind carrier frequency and timing synchronization.
Input: The observed symbols $r(k)$, $k = 0,1,...,K-1$, and frequency and timing information.
- Compute the fourth-order lag product $y(k) = r^2(k)r^2(k+1)$.
- Compute $Y(n)$ using (17).
- Estimate Ω using (23).
- Compute ε using (22) based on the target P_{fa}.
if $|Y(0)|$ or $|Y(K/2)| \geq \varepsilon$ **then**
- AL-STBC is declared present ($\mathscr{H}_1$ true).
else
- SM is declared present ($\mathscr{H}_0$ true).
end if

C. FOLP-C classification algorithm

The basic idea of the FOLP-C classification algorithm is to measure the distance between the positions of the two most

prominent peaks in $|Y(n)|$; this equals $K/2$ for the AL-STBC, whereas it does not for SM. We define n_1 as in (20), and n_2 as

$$n_2 = \arg\max_n |Y(n)|, \qquad n = 0,1,...,K-1, n \neq n_1. \tag{24}$$

If $|n_1 - n_2| = K/2$, then the AL-STBC is declared present ($\mathscr{H}_1$ true); otherwise, SM is declared present ($\mathscr{H}_0$ true).

A summary of the proposed FOLP-C algorithm is provided below.

The FOLP-C algorithm

Required signal pre-processing: Timing synchronization.
Input: The observed symbols $r(k)$, $k = 0,1,...,K-1$ and timing information.
- Compute the fourth-order lag product $y(k) = r^2(k)r^2(k+1)$.
- Compute $Y(n)$ using (17).
- $n_1 = \arg\max_n |Y(n)|, \quad n = 0,1,...,K-1.$
- $n_2 = \arg\max_n |Y(n)|, \quad n = 0,1,...,K-1, n \neq n_1.$

if $|n_1 - n_2| = K/2$ **then**
- AL-STBC is declared present ($\mathscr{H}_1$ true).

else
- SM is declared present ($\mathscr{H}_0$ true).

end if

V. Simulation Results

A. Simulation setup

The performance of the proposed algorithms was evaluated using Monte Carlo simulations with 1000 trials employed for each scenario. Unless otherwise indicated, QPSK modulation was used, $K = 1024$, $P_{fa} = 10^{-2}$ for the FOLP-B classification algorithm, and the received signal was affected by AWGN with variance σ_w^2 and a frequency-flat Nakagami-m fading channel [36], with $m = 3$, and $\mathrm{E}\{|h_i^2|\} = 1$, $i = 0,1$. Under the assumption of unit variance constellations, the SNR was defined as $10\log_{10}(N_t/\sigma_w^2)$. Two performance measures, the probability of correct classification, $P(\lambda = \xi|\xi)$, $\xi \in \{\text{SM, AL}\}$, and the average probability of correct classification, given in (14), were used.

.

B. Performance evaluation

Fig. 4 shows the analytical and simulation results for the probability of correct classification achieved with the FOM-based classification algorithm over Nakagami-m fading channel for $m = 3$ and 1. Note that the simulation and theoretical results are in very good agreement. The performance deteriorates as the effect of the channel increases. The explanation is that the increase in the variance of h_0 and h_1 with decreasing m leads to an increase in the variance of $\hat{m}_{r,4,0}$ and contributes to erroneous decisions.

The probability of correct classification for the three proposed FOLP-based classification algorithms over Nakagami-m fading channel, $m = 3$ and 1, is presented in Fig. 5. Note that for all FOLP-based algorithms, the channel parameter m and SNR affect the probability of correct classification for the AL-STBC, $P(\lambda = \text{AL}|\text{AL})$, but do not for SM. In general, the noise components and the channel coefficients control the peaks that appear in $|Y^{\text{AL}}(n)|$ at $n = 0, K/2$, as can

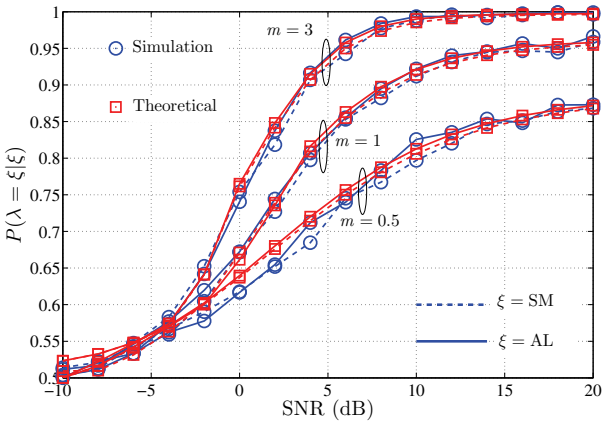

Fig. 4. Probability of correct classification, $P(\lambda = \xi|\xi)$, $\xi \in \{\text{SM, AL}\}$, versus SNR for different Nakagami-m fading channels, for the FOM-based classification algorithm with QPSK modulation and $K = 1024$.

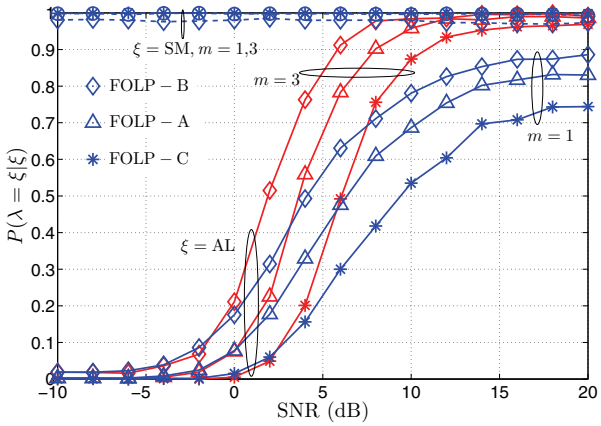

Fig. 5. Probability of correct classification, $P(\lambda = \xi|\xi)$, $\xi \in \{\text{SM, AL}\}$, versus SNR for different Nakagami-m fading channels, for the FOLP-based classification algorithms with QPSK modulation and $K = 1024$. $P_{fa} = 10^{-2}$ for the FOLP-B classification algorithm. Solid lines are used for $P(\lambda = \text{AL}|\text{AL})$ and dashed lines for $P(\lambda = \text{SM}|\text{SM})$.

be seen from (19). For the SM, $Y^{\text{SM}}(n), n = 0,1,...,K-1$, can be shown to be statistically independent and identically distributed. Accordingly, the peak of $|Y^{\text{SM}}(n)|$ can occur at any position n with the same probability, i.e., $P(|Y(0)| = \max|Y(n)|) = P(|Y(K/2)| = \max|Y(n)|) = 1/K$, regardless of the channel parameter m and noise power. Recall that, for the FOLP-A algorithm, SM is not declared present if the maximum occurs either at $n = 0$ or $K/2$. Hence, $P(\lambda = \text{SM}|\text{SM}) = 1 - 2/K$ and this approaches one for large K. For the FOLP-C algorithm, SM is not declared present if $|n_1 - n_2| = K/2$, with n_1 and n_2 defined by (20) and (24), respectively. In this case, $P(\lambda = \text{SM}|\text{SM}) = (K-2)/(K-1)$, which also approaches one for large K. On the other hand, for the FOLP-B classification algorithm, the probability of correctly classifying SM is predetermined by the probability of false alarm, i.e., $P(\lambda = \text{SM}|\text{SM}) = 1 - 2P_{fa}$, which is independent of SNR and m. It is noteworthy that the results of this analysis agree with simulation findings shown in Fig. 5.

TABLE II
COMPUTATIONAL COST OF THE PROPOSED ALGORITHMS AND THOSE IN [21] AND [26].

Classification algorithm	Computational cost (flops)	Number of flops for $K = 1024$, $M = 4$, $\rho = 4$, and $\mathscr{W} = 100$
Optimal likelihood [21]	$240KM^2$	3,932,160
Cyclostionarity [26]	$18\rho K + 5\rho K \log_2 \rho K + 27\mathscr{W}$	322,188
FOM	$20K + 233$	20,713
FOLP-A	$22K + 5K \log_2 K$	73,728
FOLP-B	$22K + 5K \log_2 K$	73,728
FOLP-C	$23K + 5K \log_2 K$	74,752

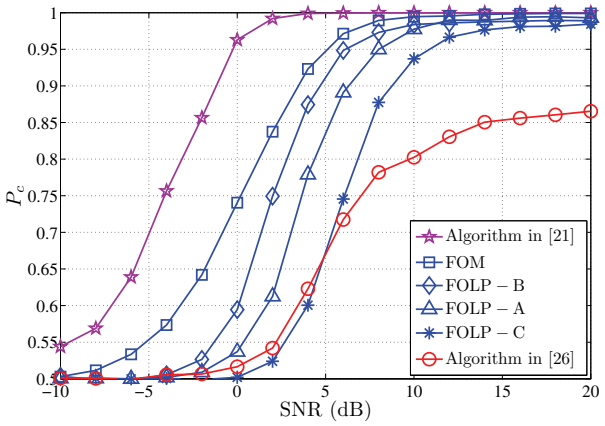

Fig. 6. Performance comparison of the proposed algorithms and the ones in [21] and [26] over Nakagami-m fading channel, $m = 3$, with QPSK modulation, $K = 1024$.

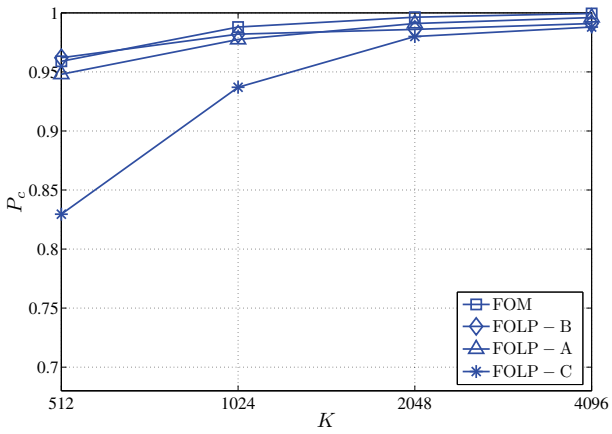

Fig. 7. The effect of K on the average probability of correct classification, P_c, for the proposed algorithms over Nakagami-m channel, $m = 3$, with QPSK modulation at SNR = 10 dB. $P_{fa} = 10^{-2}$ for the FOLP-B classification algorithm.

C. Performance comparison

Fig. 6 compares the average probability of correct classification, P_c, achieved by the proposed algorithms, the optimal likelihood-based algorithm in [21], and the cyclostionarity-based algorithm in [26]. An oversampling factor $\rho = 4$ and a window size $\mathscr{W} = 100$ are used with the algorithm in [26]. $P_{fa} = 10^{-2}$ for both FOLP-B classification algorithm and the algorithm in [26]. As expected, the algorithm in [21] provides the best performance, as it exploits the full probability density function of the received signal[5]. Furthermore, the FOM-based classification algorithm outperforms the FOLP-based algorithms, since it uses the LRT to make the decision. On the other hand, the algorithm in [26] has the lowest performance, as accurate estimation of the fourth-order cyclic cumulant requires a relatively large observation period. For example, we observed that the values obtained for P_c showed a strong dependence on K, ranging from $P_c = 0.96$ for $K = 4096$ to $P_c = 0.86$ for $K = 1024$ at SNR= 20 dB.

Additionally, the computational cost measured by the required number of floating point operations (flops) [37] is provided in Table II for the proposed algorithms and those described in [21] and [26]. As can be seen, the FOM-based algorithm has the lowest computational cost followed by the FOLP-based algorithms. The computational cost of the algorithms in [21] and [26] is considerably higher.

[5]However, it is well known that this approach heavily relies on preprocessing, is sensitive to model mismatches, and is computationally complex.

D. Effect of the number of observed samples

Fig. 7 illustrates the effect of the number of received samples, K, on the average probability of correct classification, P_c, for the proposed classification algorithms at SNR=10 dB. Note that the performance improves with increasing K. This can be explained as follows. For the FOM-based classification algorithm, the estimate of the fourth-order moment improves as K increases, thus improving the probability of correct classification. On the other hand, for the FOLP-based classification algorithms, the noise contributions that affect the peaks in $|Y^{\mathrm{AL}}(n)|$ at $n = 0, K/2$ decrease with increasing K, thus improving the classification performance for the AL-STBC. The SM classification performance approaches unity for sufficiently large K for the FOLP-A and FOLP-C algorithms, but is relatively insensitive to K for the FOLP-B algorithm. Overall, the classification performance improves with increasing K. Furthermore, Fig. 7 indicates that low values of K have a particularly adverse effect on the FOLP-C algorithm. The explanation is that the FOLP-C algorithm requires the detection of two peaks (see (20) and (24)) to classify the AL-STBC with, whereas the detection of either of the two peaks is sufficient for the FOLP-A and FOLP-B algorithms.

E. Effect of the modulation type

Fig. 8 depicts the effect of the modulation type on the average probability of correct classification, P_c, for the proposed

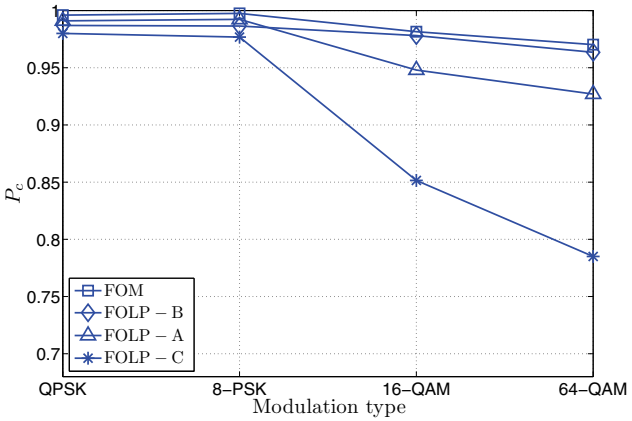

Fig. 8. The effect of the modulation type on the average probability of correct classification, P_c, for the proposed algorithms over the Nakagami-m channel, $m=3$, with $K=2048$ at SNR = 10 dB. $P_{fa}=10^{-2}$ for the FOLP-B classification algorithm.

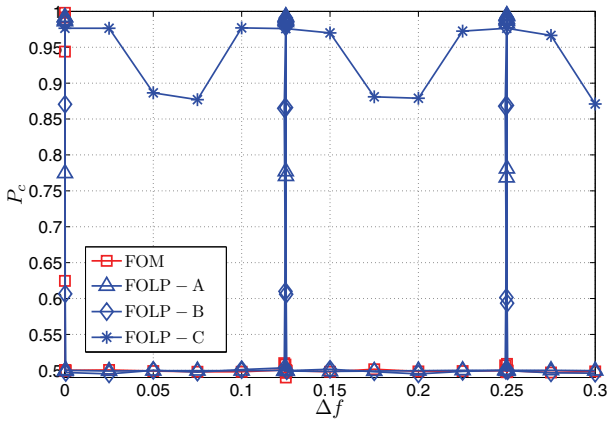

Fig. 9. The effect of the frequency offset on the average probability of correct classification, P_c, for the proposed algorithms over Nakagami-m channel, $m=3$, with QPSK modulation and $K=2048$ at SNR = 10 dB. $P_{fa}=10^{-2}$ for the FOLP-B classification algorithm.

algorithms at SNR=10 dB, and $K=2048$. The explanation for the dependence of the classification performance on the modulation type is as follows. According to Section III, the performance of the FOM-based algorithm is determined by the Euclidean distance between zero and $h_0^2h_1^2c_{x,4,2}$, with the classification performance improving as the distance increases. This distance does not depend on the M-PSK constellation, i.e., $c_{x,4,2}$ is independent of M, whereas for the M-QAM constellations, it decreases as M increases. For the FOLP-based algorithms, classification of SM is not affected by the modulation type (this can be seen from the previous discussion on $P(\lambda=\text{SM}|\text{SM})$). On the other hand, classification of the AL-STBC is independent of M for the M-PSK constellations, whereas this depends on M for M-QAM constellations. This is because the peaks in $|Y^{\text{AL}}(n)|$ at $n=0,K/2$ depend on $c_{x,4,2}$.

F. Effect of the frequency offset

Fig. 9 presents the effect of the frequency offset normalized with respect to the data rate, Δf, on the average probability of correct classification, P_c, for the proposed algorithms at SNR=10 dB and $K=2048$. These results show that the FOM-based classification algorithm is sensitive to Δf. This behavior is consistent with the analysis in the Appendix, where it is shown that a frequency offset affects the FOM of the AL-STBC signal. The performance of the FOLP-A and FOLP-B algorithms is also affected by Δf. The explanation is that Δf introduces a shift in the peaks in $\left|Y^{\text{AL}}(n)\right|$, $n=0,K/2$, except for the cases where Δf is an integer multiple of $1/8$ (see Appendix for the proof), and the decision criteria rely on the presence of a peak either at $n=0$ or $n=K/2$. On the other hand, the performance of the FOLP-C algorithm is relatively insensitive to the frequency offset. This is because the decision criterion depends on the distance between the peak positions, which is unaffected by Δf (see Appendix for the proof). Nevertheless, some performance degradation results when the shifted positions are misaligned with the DFT bins, since the peak values are attenuated (see Appendix for the proof).

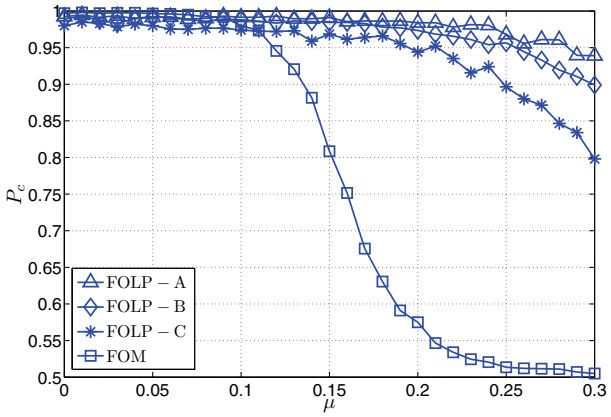

Fig. 10. The effect of the timing offset on the average probability of correct classification, P_c, over Nakagami-m channel, $m=3$, with QPSK modulation and $K=2048$ at SNR = 10 dB. $P_{fa}=10^{-2}$ for the FOLP-B classification algorithm.

G. Effect of the timing offset

The previous analysis assumed perfect timing synchronization. Here we evaluate the performance of the proposed algorithms in the presence of a timing offset, $0\leq\mu<1$. For the case of rectangular pulse shaping, after the matched filtering, the timing offset, μ, translates into a two path channel $[1-\mu,\mu]$ [11]. Fig. 10 shows the performance of the proposed algorithms as a function of μ at SNR=10 dB and $K=2048$. The FOLP-based algorithms display much less sensitivity to timing offsets than the FOM-based algorithm.

H. Effect of the spatially correlated fading

Independent fading was considered in the previous analysis. Here we show the effect of correlated fading on the classification performance. Correlated Nakagami-m fading was generated using correlated complex-valued Gaussian variables ([38], p. 25), the inverse cumulative distribution function (cdf) method [36], and an approximation of the Nakagami-m inverse cdf [36]. Fig. 11 shows the average probability

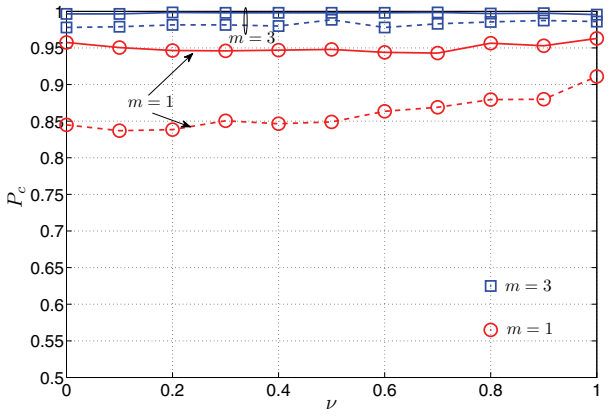

Fig. 11. The effect of the spatial correlation between transmitted antennas on the average probability of correct classification, P_c, for the FOM and FOLP-C classification algorithms over Nakagami-m fading channel, $m=3$ and 1, with QPSK modulation and $K=2048$ at SNR=10 dB. Solid lines are used for the FOM-based algorithm and dashed lines for the FOLP-C algorithm.

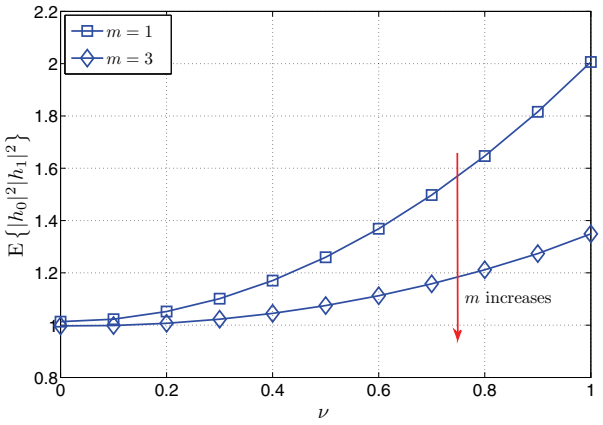

Fig. 12. $\mathrm{E}\{|h_0|^2|h_1|^2\}$ versus the correlation coefficient, ν, for Nakagami-m fading channel, $m=3$ and 1.

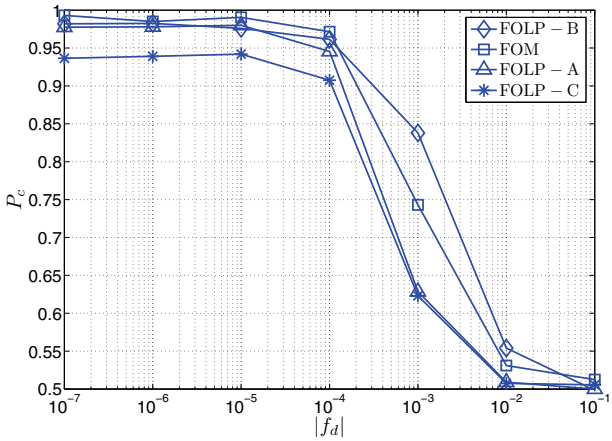

Fig. 13. The effect of the Doppler frequency on the average probability of correct identification, P_c, for the proposed identification algorithms over Nakagami-m fading channel, $m=3$, with QPSK modulation and $K=1024$ at SNR=10 dB.

of correct classification, P_c, of the FOM-based and FOLP-C algorithms versus the correlation coefficient between h_0 and h_1, ν, over Nakagami-m fading with $m=3$ and 1, for the QPSK modulation at SNR=10 dB and $K=2048$. Note that the performance improves as ν increases, especially at lower values of m [6]. This can be explained as follows. We recall that, for the AL-STBC, $|m_{r,4,0}|$, which controls the performance of the FOM-based algorithm, and the absolute value of the DFT peak, $|\mathscr{E}|$, which controls the performance of the FOLP-based algorithms, are proportional to $\left|h_0^2 h_1^2\right|$ (as shown in (5) and Section IV). For SM, these two parameters are zero valued if the noise contributions are neglected. The question arises how the spatial correlation between the two channels affects $\left|h_0^2 h_1^2\right|$. Fig. 12, which shows $\mathrm{E}\{|h_0|^2|h_1|^2\}$ as a function of ν for different values of m, helps us to answer this question. Note that since h_0 and h_1 change their values randomly from one realization to another, we resort to the statistical mean value, $\mathrm{E}\{|h_0|^2|h_1|^2\}$, instead of the instantaneous value, $\left|h_0^2 h_1^2\right|$. It is obvious from Fig. 12 that $\mathrm{E}\{|h_0|^2|h_1|^2\}$ is an increasing function of ν. This explains why the classification performance improves with ν for $m=1$, as shown in Fig. 11. However, for $m=3$, there is not much improvement in the classification performance. This is because the classification performance at $\nu=0$ is high enough and $\mathrm{E}\{|h_0|^2|h_1|^2\}$ increases slowly with ν. This agrees with the fact that in the case of no fading (m tends to infinity), $\mathrm{E}\{|h_0|^2|h_1|^2\}$ is essentially independent of ν.

I. Effect of the Doppler frequency

The previous analysis assumed constant channel coefficients over the observation period. Here we consider the effect of the Doppler frequency on the performance of the proposed algorithms. Fig. 13 shows the average probability of correct classification, P_c, for the FOM- and FOLP-based algorithms versus the Doppler frequency magnitude normalized to the data rate, $|f_d|$, at SNR= 10 dB and $K=1024$. These results show good robustness for $|f_d|<10^{-4}$.

J. Effect of the probability of false alarm

Fig. 14 presents the effect of the probability of false alarm, P_{fa}, on the probability of correct classification, $P(\lambda=\xi|\xi)$, $\xi\in\{\mathrm{SM},\mathrm{AL}\}$, for the FOLP-B classification algorithm. It is noted that the AL-STBC classification performance improves as P_{fa} increases. An increase in the P_{fa} leads to a reduction in the threshold value, and, hence, $|Y(0)|$ or $|Y(K/2)|\geq\varepsilon$ are more easily satisfied, thus leading to a better performance. On the other hand, the SM classification performance decreases with an increase in P_{fa}, as $P(\lambda=\mathrm{SM}|\mathrm{SM})=1-2P_{fa}$. Therefore, the value of P_{fa} is chosen as a trade-off between the SM and AL-STBC classification performances.

VI. Conclusion

The classification of spatial multiplexing (SM) and Alamouti space-time block code (AL-STBC) signals was investigated in this paper. It was shown that a fourth-order moment

[6]Similar results are obtained for the FOLP-A and FOLP-B algorithms; however, these results were omitted due to space considerations.

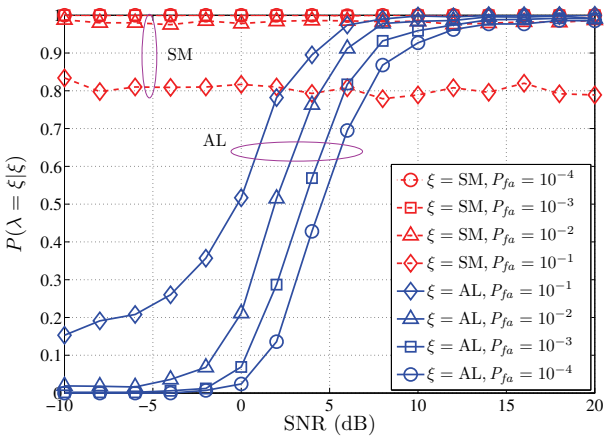

Fig. 14. The effect of P_{fa} on the probability of correct classification, $P(\lambda = \xi|\xi)$, $\xi \in \{\text{SM, AL}\}$, for the FOLP-B classification algorithm over Nakagami-m channel, $m = 3$, with QPSK modulation and $K = 1024$.

(FOM) and the discrete Fourier transform (DFT) of a fourth-order lag product (FOLP) can be used as discriminating signal features. Based on these results, four novel classification algorithms were proposed. The first algorithm employs the FOM of the received signal as a discriminating feature and the likelihood ratio test (LRT) to make a decision. Analytical results for the algorithm classification performance were derived. However, the practical implementation of this algorithm is complicated by the need for channel estimation, modulation classification, and noise power estimation. To relax these requirements, we proposed three algorithms based on the DFT of the received signal FOLP, namely FOLP-A, FOLP-B, and FOLP-C. The influence of model mismatches (e.g., frequency and timing offsets, Doppler frequency, and spatially correlated fading) on the performance of the proposed algorithms was also investigated. Unlike the FOM-based, FOLP-A, and FOLP-B algorithms, FOLP-C is robust with respect to frequency offsets. Furthermore, the FOLP-based algorithms have lower sensitivity to the timing offset when compared to the FOM-based algorithm. The proposed algorithms are tolerant to a Doppler frequency whose magnitude, normalized with respect to the data rate, is lower than 10^{-4}. Also, their performance can benefit from spatially correlated fading. As part of future work, we plan to extend the proposed classification algorithms to a larger pool of STBCs.

APPENDIX

Effect of the frequency offset on the discriminating signal features

The effects of a frequency offset on the proposed discriminating signal features have been determined. In the presence of such an offset, the received signal, $r'(k)$ is

$$r'(k) = r(k)e^{-j(2\pi\Delta fk)}, \qquad k = 0,1,...,K-1, \qquad (25)$$

where $r(k)$ is given in (3) and Δf represents the frequency offset normalized to the data rate.

Effect on the FOM-based feature

In the presence of a frequency offset, the estimated fourth-order moment, $\hat{m}_{r',4,0}$, is given by

$$\begin{aligned}\hat{m}_{r',4,0} &= \frac{1}{K}\sum_{k=0}^{K-1} r'^2(k)r'^2(k+1) \\ &= e^{-j(4\pi\Delta f)}\left[\frac{1}{K}\sum_{k=0}^{K-1} r^2(k)r^2(k+1)e^{-j(8\pi\Delta fk)}\right]. \qquad (26)\end{aligned}$$

The discrete-time Fourier transform of the sequence $y(k) = r^2(k)r^2(k+1), k = 0,1,...,K-1$, can be computed as,

$$\mathscr{Y}(f) = \sum_{k=0}^{K-1} r^2(k)r^2(k+1)e^{-j(2\pi fk)}, \quad 0 \le f \le 1. \qquad (27)$$

From (26) and (27), it is clear that $\hat{m}_{r',4,0} = e^{-j(4\pi\Delta f)}\left[\frac{1}{K}\mathscr{Y}(4\Delta f)\right]$. If $K \to \infty$, the noise components $\psi^{\text{SM}}(k)$ and $\psi^{\text{AL}}(k)$ in (15) and (16) vanish, with the result that $\mathscr{Y}(f) = K(h_0^2h_1^2c_{x,4,2})[\delta(f) + \delta(f-1/2)]$ for the AL STBC, while $\mathscr{Y}(f) = 0$ for the SM. Under such conditions, it follows that, for the AL STBC, $\hat{m}_{r',4,0} = m_{r',4,0} = m_{r,4,0} = h_0^2h_1^2c_{x,4,2}$ if $\Delta f = 0$, $\hat{m}_{r',4,0} = m_{r',4,0} = -jh_0^2h_1^2c_{x,4,2}$ if $\Delta f = 0.125$, and $\hat{m}_{r',4,0} = 0$ otherwise, whereas for the SM $\hat{m}_{r',4,0} = m_{r',4,0} = m_{r,4,0} = 0$ regardless of Δf. As such, the classification of AL STBC is affected by Δf.

Effect on the FOLP-based feature

The FOLP in the presence of the frequency offset can be calculated as,

$$\begin{aligned}y'(k) &= r'^2(k)r'^2(k+1) \\ &= e^{-j(4\pi\Delta f)}r^2(k)r^2(k+1)e^{-j(8\pi\Delta fk)}, \quad k = 0,1,...,K-1. \qquad (28)\end{aligned}$$

Taking the K-point DFT of (28) yields

$$\begin{aligned}Y'(n) &= \frac{1}{\sqrt{K}}\sum_{k=0}^{K-1} y'(k)e^{-j(2\pi kn/K)} \\ &= e^{-j(4\pi\Delta f)}\left[\frac{1}{K}\sum_{k=0}^{K-1} r^2(k)r^2(k+1)e^{-j2\pi k(n+4K\Delta f)/K}\right]. \qquad (29)\end{aligned}$$

Since the decision is taken according to $|Y'(n)|$, the term $e^{-j(4\pi\Delta f)}$ has no effect. By using the shift property of the DFT, we obtain

$$|Y'(n)| = \mathscr{A}(n)|Y(n + \lceil 4K\Delta f \rfloor)|, \qquad (30)$$

where $\lceil . \rfloor$ denotes the rounding function and $\mathscr{A}(n)$ represents an attenuation factor, which can be calculated as,

$$\mathscr{A}(n) = \frac{1}{|Y(n)|}\left|\frac{1}{\sqrt{K}}\sum_{k=0}^{K-1} y(k)e^{-j2\pi k(n+[\lceil 4K\Delta f\rfloor - 4K\Delta f])/K}\right|. \qquad (31)$$

Examination of (30) shows that the peaks $|Y(0)|$ and $|Y(K/2)|$ for the AL STBC are shifted by $\lceil 4K\Delta f \rfloor$ and their

magnitudes are scaled by $\mathscr{A}(0)$ and $\mathscr{A}(K/2)$, respectively. If Δf is an integer multiple of $1/8$, it is straightforward to show that the peaks are circularly shifted by $K/2$, with the result that their positions are unchanged. Furthermore, note that $\mathscr{A}(n)$ equals one if Δf is an integer multiple of $1/4K$; otherwise, $\mathscr{A}(n)$ is less than one.

ACKNOWLEDGEMENT

The authors are grateful to the anonymous reviewers and the Editor, Dr. C. da Silva, for their constructive comments.

REFERENCES

[1] B. Wang and K. J. R. Liu, "Advances in cognitive radio networks: a survey," *IEEE J. Sel. Topics Signal Process.*, vol. 5, pp. 5–23, Feb. 2011.
[2] A. B. MacKenzie *et al.*, "Cognitive radio and networking research at Virginia Tech," *Proc. IEEE*, vol. 97, pp. 660–688, Apr. 2009.
[3] D. Cabric, "Cognitive radios: system design perspective," Ph.D. dissertation, University of California, Berkeley, USA, 2007.
[4] D. Cabric, S. Mishra, and R. Brodersen, "Implementation issues in spectrum sensing for cognitive radios," in *Proc. 2004 IEEE ASILOMAR*, pp. 772–776.
[5] T. Yucek and H. Arslan, "A survey of spectrum sensing algorithms for cognitive radio applications," *IEEE Commun. Surveys & Tutorials*, vol. 11, pp. 116–130, Mar. 2009.
[6] Y. Zheng, Y.-C. Liang, A. T. Hoang, and R. Zhang, "A review on spectrum sensing for cognitive radio: challenges and solutions," *EURASIP J. Adv. Signal Process.*, DOI:10.1155/2010/381465, 2010.
[7] E. Axell, G. Leus, E. Larsson, and H. Poor, "Spectrum sensing for cognitive radio: state-of-the-art and recent advances," *IEEE Signal Process. Mag.*, vol. 29, pp. 101–116, May 2012.
[8] O. A. Dobre, A. Abdi, Y. Bar-Ness, and W. Su, "A survey of automatic modulation classification techniques: classical approaches and new developments," *IET Commun.*, vol. 1, pp. 137–156, Apr. 2007.
[9] H.-C. Wu, M. Saquib, and Z. Yun, "Novel automatic modulation classification using cumulant features for communications via multipath channels," *IEEE Trans. Wireless Commun.*, vol. 7, pp. 3098–3105, Aug. 2008.
[10] M. Oner and F. Jondral, "On the extraction of the channel allocation information in spectrum pooling systems," *IEEE J. Sel. Areas Commun.*, vol. 25, pp. 558–565, Apr. 2007.
[11] A. Swami and B. Sadler, "Hierarchical digital modulation classification using cumulants," *IEEE Trans. Commun.*, vol. 48, pp. 416–429, Mar. 2000.
[12] A. Punchihewa, Q. Zhang, O. A. Dobre, C. Spooner, S. Rajan, and R. Inkol, "On the cyclostationarity of OFDM and single carrier linearly digitally modulated signals in time dispersive channels: theoretical developments and application," *IEEE Trans. Wireless Commun.*, vol. 9, pp. 2588–2599, Aug. 2010.
[13] F. Hameed, O. A. Dobre, and D. C. Popescu, "On the likelihood-based approach to modulation classification," *IEEE Trans. Wireless Commun.*, vol. 8, pp. 5884–5892, Dec. 2009.
[14] V. G. Chavali and C. R. C. M. da Silva, "Maximum-likelihood classification of digital amplitude-phase modulated signals in flat fading non-Gaussian channels," *IEEE Trans. Commun.*, vol. 59, pp. 2051–2056, Aug. 2011.
[15] W. C. Headley and C. R. C. M. da Silva, "Asynchronous classification of digital amplitude-phase modulated signals in flat-fading channels," *IEEE Trans. Commun.*, vol. 59, pp. 7–12, Jan. 2011.
[16] A. Al-Habashna, O. A. Dobre, R. Venkatesan, and D. C. Popescu, "Second-order cyclostationarity of mobile WiMAX and LTE OFDM signals and application to spectrum awareness in cognitive radio systems," *IEEE J. Sel. Topics Sig. Proc.*, vol. 6, pp. 26–42, Feb. 2012.
[17] M. Shi, Y. Bar-Ness, and W. Su, "Adaptive estimation of the number of transmit antennas," in *Proc. 2007 IEEE MILCOM*, pp. 1–5.
[18] O. Somekh, O. Simeone, Y. Bar-Ness, and W. Su, "Detecting the number of transmit unauthorized or cognitive receivers in MIMO systems," in *Proc. 2007 IEEE MILCOM*, pp. 1–5.
[19] V. Choqueuse, S. Azou, K. Yao, and G. Burel, "Blind modulation recognition for MIMO systems," *J. Military Technical Academy Review*, vol. XIX, pp. 183–196, Jun. 2009.
[20] K. Hassan, I. Dayoub, W. Hamouda, C. Nzeza, and M. Berbineau, "Blind digital modulation identification for spatially-correlated MIMO systems," *IEEE Trans. Wireless Commun.*, vol. 11, pp. 683–693, Feb. 2012.
[21] V. Choqueuse, M. Marazin, L. Collin, K. Yao, and G. Burel, "Blind recognition of linear space time block codes: a likelihood-based approach," *IEEE Trans. Signal Process.*, vol. 58, pp. 1290–1299, Mar. 2010.
[22] V. Choqueuse, K. Yao, L. Collin, and G. Burel, "Hierarchical space-time block code recognition using correlation matrices," *IEEE Trans. Wireless Commun.*, vol. 7, pp. 3526–3534, Sep. 2008.
[23] ——, "Blind recognition of linear space time block codes," in *Proc. 2008 IEEE ICASSP*, pp. 2833–2836.
[24] M. Shi, Y. Bar-Ness, and W. Su, "STC and BLAST MIMO modulation recognition," in *Proc. 2007 IEEE GLOBECOM*, pp. 3034–3039.
[25] M. Marey, O. A. Dobre, and R. Inkol, "Classification of space-time block codes based on second-order cyclostationarity with transmission impairments," *IEEE Trans. Wireless Commun.*, vol. 11, pp. 2574–2584, Jul. 2012.
[26] M. DeYoung, R. Heath, and B. Evans, "Using higher order cyclostationarity to identify space-time block codes," in *Proc. 2008 IEEE GLOBECOM*, pp. 1–5.
[27] M. Jankiraman, *Space-Time Codes and MIMO Systems*. Artech House, 2004.
[28] V. Tarokh, H. Jafarkhani, and A. Calderbank, "Space time block codes from orthogonal designs," *IEEE Trans. Inf. Theory*, vol. 45, pp. 744–765, Jul. 1999.
[29] S. Alamouti, "A simple transmit diversity technique for wireless communications," *IEEE J. Sel. Areas Commun.*, vol. 16, pp. 1451–1458, Oct. 1998.
[30] J. Mendel, "Tutorial on higher-order statistics (spectra) in signal processing and system theory: theoretical results and some applications," *Proc. IEEE*, vol. 79, pp. 278–305, Mar. 1991.
[31] D. R. Brillinger, *Time Series: Data Analysis and Theory*. McGraw-Hill, 1981.
[32] J. G. Proakis and M. Salehi, *Communication Systems Engineering*. Prentice Hall, 2002.
[33] P. J. Davis and P. Rabinowitz, *Methods of Numerical Integration*. Academic Press, 1975.
[34] H. Van Trees, *Detection, Estimation, and Modulation Theory: Detection, Estimation, and Linear Modulation Theory*. Wiley, 2001.
[35] A. Papoulis and S. Pillai, *Probability, Random Variables and Stochastic Processes*. McGraw-Hill, 2001.
[36] N. Beaulieu and C. Cheng, "Efficient Nakagami-m fading channel simulation," *IEEE Trans. Veh. Technol.*, vol. 54, pp. 413–424, Mar. 2005.
[37] D. Watkins, *Fundamentals of Matrix Computations*. Wiley, 2002.
[38] M. E. Johnson, *Multivariate Statistical Simulation*. Wiley, 1987.

Yahia A. Eldemerdash received the B.Sc. and M.Sc. degrees in Electrical and Computer Engineering from Al-Azhar University, Cairo, Egypt, in 2002 and 2007, respectively. Between 2003 and 2010, he was a Research and Teaching Assistant at the National Telecommunication Institute in Cairo. He is currently working towards the Ph.D. degree with the Faculty of Engineering and Applied Science at Memorial University, Canada. His research interests lie in the areas of wireless communications and signal processing, with particular emphasis on space-time coding, blind signal classification, blind parameter estimation, and spectrum sensing for cognitive radio.

Mohamed Marey received the M.Sc. and Ph.D. degrees in Electrical Engineering from Menoufyia University, Egypt, and Ghent University, Belgium, in 1999 and 2008, respectively. Previously, he joined the Faculty of Engineering and Applied Science, Memorial University, Canada, as a postdoctoral fellow. Currently, he is as an Assistant Professor at the Department of Electronic and Communication Engineering, Menoufyia University. Dr. Marey received the young scientist award from International Union of Radio Science (URSI) in 1999. He is the author of the book *MultiCarrier Receivers in the Presence of Interference: Overlay Systems* (VDM Publishing House Ltd., 2009), and approximately 40 scientific papers published in international journals and conferences. His main research interests are in wireless communications and digital signal processing, with a particular focus on: cooperative communications, cognitive radio systems, multiple-input multiple-output antenna systems, multi-carrier systems, synchronization and channel estimation, and error correcting codes.

Octavia A. Dobre received the Dipl. Ing. and Ph. D. degrees in ECE from the Polytechnic University of Bucharest (formerly the Polytechnic Institute of Bucharest), Romania, in 1991 and 2000, respectively. In 2001 she held a Fulbright fellowship at Stevens Institute of Technology, USA. Between 2002 and 2005, she was a Research Associate with New Jersey Institute of Technology, USA. Since 2005 she has been with the Faculty of Engineering and Applied Science at Memorial University, Canada, where she is currently an Associate Professor. Her research interests include cognitive radio systems, spectrum sensing techniques, blind signal classification and parameter estimation techniques, transceiver optimization algorithms, dynamic spectrum access, cooperative wireless communications, network coding, and resource allocation. Dr. Dobre published over 100 journal and conference papers in these areas. She is an Editor for the IEEE COMMUNICATIONS LETTERS, IEEE COMMUNICATIONS SURVEYS AND TUTORIALS, and *Elsevier PHYCOM*, and served as a Guest Editor for the IEEE JOURNAL OF SELECTED TOPICS ON SIGNAL PROCESSING and Lead Guest Editor of the *Elsevier PHYCOM* "Cognitive Radio: The Road for its Second Decade" special issue. She is the Co-Chair for the IEEE ICC 2013 and IEEE GLOBECOM 2013 (Signal Processing for Communications Symposium), and IEEE VTC Spring 2013 (Multiple Antenna Systems and Services Track).

George K. Karagiannidis was born in Pithagorion, Samos Island, Greece. He received the University Diploma (5 years) and Ph.D degree, both in electrical and computer engineering from the University of Patras, in 1987 and 1999, respectively. From 2000 to 2004, he was a Senior Researcher at the Institute for Space Applications and Remote Sensing, National Observatory of Athens, Greece. In June 2004, he joined the faculty of Aristotle University of Thessaloniki, Greece where he is currently Director of Digital Telecommunications Systems and Networks Laboratory. His research interests are in the broad area of digital communications systems with emphasis on communications theory, energy efficient MIMO and cooperative communications, cognitive radio, smart grid and optical wireless communications.

He is the author or co-author of more than 180 technical papers published in scientific journals and presented at international conferences. He is also author of the Greek edition of a book on *Telecommunications Systems* and co-author of the book *Advanced Wireless Communications Systems* (Cambridge Publications, 2012). He is co-recipient of the Best Paper Award of the Wireless Communications Symposium (WCS) in the IEEE International Conference on Communications (ICC'07), Glasgow, U.K., June 2007.

Dr. Karagiannidis has been a member of Technical Program Committees for several IEEE conferences such as ICC, GLOBECOM, VTC, etc. In the past he was Editor for Fading Channels and Diversity of the IEEE TRANSACTIONS ON COMMUNICATIONS, Senior Editor of IEEE COMMUNICATIONS LETTERS and Editor of the *EURASIP Journal of Wireless Communications & Networks*. He was Lead Guest Editor of the special issue on "Optical Wireless Communications of the IEEE JOURNAL ON SELECTED AREAS IN COMMUNICATIONS and Guest Editor of the special issue on "Large-scale multiple antenna wireless systems." Since January 2012, he is the Editor-in Chief of the IEEE COMMUNICATIONS LETTERS.

Robert Inkol received the B.Sc. and M.A.Sc. degrees in Applied Physics and Electrical Engineering from the University of Waterloo in 1976 and 1978, respectively. From 1978 to 2012, he was a Defence Scientist with Defence Research and Development Canada (DRDC) where he was responsible for the technical leadership of various electronic warfare related projects and research programs. He was responsible for numerous contributions to the application of very large scale integrated circuit technology and digital signal processing techniques to electronic warfare systems. In addition to having produced numerous publications, Mr. Inkol holds four patents. He is a Senior Member of IEEE, and has served as a reviewer for various publications and as a Technical Program Committee member for several IEEE conferences. Recently, he received the Queen Elizabeth II Diamond Jubilee medal for his contributions to DRDC. He is currently an Adjunct Professor at the Royal Military College of Canada.